



Article scientifique

Article

2005

Published version

Open Access

This is the published version of the publication, made available in accordance with the publisher's policy.

---

## The 1.3 Å crystal structure of the flavoprotein YqjM reveals a novel class of Old Yellow Enzymes

---

Kitzing, Karina; Fitzpatrick, Thérèse Bridget; Wilken, Corinna; Sawa, Justyna; Bourenkov, Gleb P; Macheroux, Peter; Clausen, Tim

### How to cite

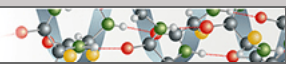
KITZING, Karina et al. The 1.3 Å crystal structure of the flavoprotein YqjM reveals a novel class of Old Yellow Enzymes. In: The Journal of biological chemistry, 2005, vol. 280, n° 30, p. 27904–27913. doi: 10.1074/jbc.M502587200

This publication URL: <https://archive-ouverte.unige.ch/unige:89528>

Publication DOI: [10.1074/jbc.M502587200](https://doi.org/10.1074/jbc.M502587200)

**Protein Structure and Folding:**  
**The 1.3 Å Crystal Structure of the  
Flavoprotein YqjM Reveals a Novel Class  
of Old Yellow Enzymes**

PROTEIN STRUCTURE  
AND FOLDING



Karina Kitzing, Teresa B. Fitzpatrick, Corinna  
Wilken, Justyna Sawa, Gleb P. Bourenkov,  
Peter Macheroux and Tim Clausen  
*J. Biol. Chem.* 2005, 280:27904-27913.

doi: 10.1074/jbc.M502587200 originally published online May 12, 2005

---

Access the most updated version of this article at doi: [10.1074/jbc.M502587200](https://doi.org/10.1074/jbc.M502587200)

Find articles, minireviews, Reflections and Classics on similar topics on the [JBC Affinity Sites](#).

Alerts:

- [When this article is cited](#)
- [When a correction for this article is posted](#)

[Click here](#) to choose from all of JBC's e-mail alerts

This article cites 32 references, 9 of which can be accessed free at  
<http://www.jbc.org/content/280/30/27904.full.html#ref-list-1>

# The 1.3 Å Crystal Structure of the Flavoprotein YqjM Reveals a Novel Class of Old Yellow Enzymes\*

Received for publication, March 8, 2005, and in revised form, April 13, 2005  
Published, JBC Papers in Press, May 12, 2005, DOI 10.1074/jbc.M502587200

Karina Kitzing<sup>‡§</sup>, Teresa B. Fitzpatrick<sup>¶</sup>, Corinna Wilken<sup>‡</sup>, Justyna Sawa<sup>‡</sup>, Gleb P. Bourenkov<sup>||</sup>, Peter Macheroux<sup>\*\*</sup>, and Tim Clausen<sup>‡§</sup>

From the <sup>‡</sup>Research Institute of Molecular Pathology (IMP), Dr. Bohr-Gasse 7, A-1030 Vienna, Austria, the <sup>¶</sup>Eidgenössische Technische Hochschule (ETH) Zürich, Institut für Pflanzenwissenschaften, Universitätsstrasse 2, CH-8092 Zürich, Switzerland, the <sup>||</sup>Max-Planck-Arbeitsgruppen für Strukturelle Molekularbiologie, Deutsches Elektronen-Synchrotron, Notkestrasse 85, D-22603 Hamburg, Germany, and the <sup>\*\*</sup>Technische Universität Graz, Institut für Biochemie, Petersgasse 12/II, A-8010 Graz, Austria

Here we report the crystal structure of YqjM, a homolog of Old Yellow Enzyme (OYE) that is involved in the oxidative stress response of *Bacillus subtilis*. In addition to the oxidized and reduced enzyme form, the structures of complexes with *p*-hydroxybenzaldehyde and *p*-nitrophenol, respectively, were solved. As for other OYE family members, YqjM folds into a ( $\alpha/\beta$ )<sub>8</sub>-barrel and has one molecule of flavin mononucleotide bound non-covalently at the COOH termini of the  $\beta$ -sheet. Most of the interactions that control the electronic properties of the flavin mononucleotide cofactor are conserved within the OYE family. However, in contrast to all members of the OYE family characterized to date, YqjM exhibits several unique structural features. For example, the enzyme exists as a homotetramer that is assembled as a dimer of catalytically dependent dimers. Moreover, the protein displays a shared active site architecture where an arginine finger (Arg<sup>336</sup>) at the COOH terminus of one monomer extends into the active site of the adjacent monomer and is directly involved in substrate recognition. Another remarkable difference in the binding of the ligand in YqjM is represented by the contribution of the NH<sub>2</sub>-terminal Tyr<sup>28</sup> instead of a COOH-terminal tyrosine in OYE and its homologs. The structural information led to a specific data base search from which a new class of OYE oxidoreductases was identified that exhibits a strict conservation of active site residues, which are critical for this subfamily, most notably Cys<sup>26</sup>, Tyr<sup>28</sup>, Lys<sup>109</sup>, and Arg<sup>336</sup>. Therefore, YqjM is the first representative of a new bacterial subfamily of OYE homologs.

YqjM from the soil bacterium *Bacillus subtilis* is a member of the Old Yellow Enzyme (OYE)<sup>1</sup> family of flavin oxidoreductases

\* This work was supported in part by Grant No. 17215 from the Austrian Science Fund (FWF) (to P. M.). The research at the Research Institute of Molecular Pathology (Vienna, Austria) was funded by Boehringer Ingelheim. The costs of publication of this article were defrayed in part by the payment of page charges. This article must therefore be hereby marked "advertisement" in accordance with 18 U.S.C. Section 1734 solely to indicate this fact.

The atomic coordinates and structure factors (code 1Z41 (unliganded oxidized YqjM), 1Z48 (unliganded reduced YqjM), 1Z42 (complex structure with *p*-hydroxybenzaldehyde), and 1Z44 (complex structure with *p*-nitrophenol)) have been deposited in the Protein Data Bank, Research Collaboratory for Structural Bioinformatics, Rutgers University, New Brunswick, NJ (<http://www.rcsb.org/>).

§ To whom correspondence may be addressed. Tel.: 43-1-79730482; Fax: 43-1-7987153; E-mail: kitzingk@gmx.net (for K. K.) or clausen@imp.univie.ac.at (for T. C.).

<sup>1</sup> The abbreviations used are: OYE, Old Yellow Enzyme; FMN, flavin mononucleotide; pHBA, *p*-hydroxybenzaldehyde; pNP, *p*-nitrophenol; SeMet, selenomethionine; SAD, single-wavelength anomalous

diffraction; PETN, pentaerythritol tetranitrate; r.m.s.d., root mean square deviation; MR, morphinone reductase; OPR, 12-oxophytodienoate reductase.

as inferred by sequence comparison and detailed biochemical investigations (1). OYE itself is an enzyme of significant historical importance, since studies performed with OYE revolutionized the whole field of enzymatic catalysis, thereby highlighting the importance of small vitamin-derived molecules that act as enzymatic cofactors or prosthetic groups. OYE was first isolated in 1932 from brewers' bottom yeast by Warburg and Christian (2), and was found to contain a non-covalently bound flavin mononucleotide (FMN). Hugo Theorell (3–5) then went on to demonstrate that the reaction catalyzed by OYE is strictly dependent on this vitamin B<sub>2</sub> (riboflavin) derivative. Consequently he postulated one of the main paradigms in biochemistry: neither apoprotein nor cofactor alone can catalyze the corresponding redox reaction, and only both together yield the active holoenzyme. Intensive studies on OYE spanning more than 70 years contributed greatly to enhancing the general understanding of flavoenzyme catalysis. More specifically, in the so-called reductive half-reaction, NADPH was established to serve as reductant of FMN (6, 7). The cofactor is converted back to its original form in the oxidative half-reaction where flavin then acts as an electron donor reducing the substrate during this step.

Despite detailed investigations of OYE, the natural substrates have remained elusive for a long time. Several studies, however, showed that quinones as well as a large variety of  $\alpha,\beta$ -unsaturated aldehydes and ketones function as efficient oxidants of flavin, leading to the reduction of the olefinic bond (8, 9). Recently, two-hybrid screen studies have suggested a possible role of one OYE isozyme, OYE2 from *Saccharomyces cerevisiae*, in controlling the redox state of actin and thereby maintaining the proper plasticity of the actin cytoskeleton (10). In fact, reactive oxygen species generated after oxidative stress have been shown to react with the actin sulfhydryl groups of Cys<sup>285</sup> and Cys<sup>374</sup>. A disulfide bond is then formed, resulting in cross-linking of actin filaments (10). This actin oxidation might be prevented by the action of OYE2 that seems to function as a flavin disulfide reductase. However, OYE3, another OYE isozyme from *S. cerevisiae*, failed to interact with actin, and therefore general functional conclusions for the whole OYE family cannot be drawn. The findings from Haarer and Amberg (10) do, however, confirm former observations that OYE serves as a detoxification enzyme in the antioxidant defense system and disarms a variety of reactive oxidative species. Among others, this has been also inferred by Fitzpatrick *et al.* (1) who demonstrated that treatment with hydrogen peroxide or nitro-

compounds such as TNT induces the expression of YqjM, an OYE homolog, from *B. subtilis*.

Data base searches have indicated that YqjM displays a high degree of sequence similarity to OYE1 from *Saccharomyces carlsbergensis* and its homologs (1). *Pseudomonas putida* Xena, a xenobiotic reductase, appears to be the closest homolog exhibiting 40% identity. Biochemical analysis of YqjM has shown that the enzyme shares some important common features with members of the OYE family (1). For example, YqjM binds the FMN cofactor non-covalently and reduces the flavin in the reductive half-reaction at the expense of NADPH. Like other members of the family, YqjM transfers electrons from the reduced flavin to the double bond of a variety of  $\alpha,\beta$ -unsaturated carbonyl compounds and accepts also electrophilic xenobiotics such as nitroglycerin, *N*-ethylmaleimide, and trinitrotoluene as substrates for the oxidative half-reaction. Finally, phenolic compounds such as *p*-hydroxybenzaldehyde (pHBA) bind tightly to this enzyme and form charge transfer complexes due to the overlapping  $\pi$ -electrons of the electron-rich phenolate ligand and the electron-deficient flavin isoalloxazine ring (1).

However, on comparing YqjM with OYE, several important differences are apparent. For example, photoreduction of YqjM leads directly to the fully reduced state; whereas in the yeast and plant homologs the red flavin semiquinone is kinetically stabilized (1). A further unique feature of YqjM is attributed to its oligomerization state. While all other OYE homologs are either monomeric or dimeric enzymes, YqjM is the only known family member that functions as a homotetramer (11) suggesting the evolution of particular residues involved in the interface formation between the protomers. This implies that the different modes of self-assembly within the OYE family may be correlated with a functional diversity. Finally, sequence comparisons have suggested significant changes in the active site of the enzyme. For example, Thr<sup>37</sup> of OYE, which regulates the redox potential of the FMN cofactor (12), is replaced by Cys<sup>26</sup> in YqjM, whereas the OYE-Tyr<sup>375</sup>, which is essential for substrate and inhibitor binding, has no conserved counterpart in YqjM.

The three-dimensional structures from OYE (13) and several of its homologs (14–17) have been elucidated and point to the fundamental fold of YqjM. However, to determine the molecular basis of the unique properties of YqjM, we solved the structures of the oxidized and reduced holoenzyme and of complexes with the inhibitors pHBA and *p*-nitrophenol (pNP), respectively. The data presented here confirm that YqjM shares the overall fold of the OYE family. Also it demonstrates unequivocally that YqjM is in fact the first characterized representative of a new class of OYE homologs showing fundamental differences to the classical OYE enzymes.

#### EXPERIMENTAL PROCEDURES

**Materials**—All materials used were of analytical grade. All chemicals were purchased from Sigma. Chromatographic columns were from Amersham Biosciences.

**Expression and Purification of the Native YqjM**—The construct of pET21a (Novagen) with the open reading frame of *yqjM* was expressed and purified as described in Ref. 1 with the following modifications: purification was performed with an AEKTA-FPLC system from Amersham Biosciences using a HiPrep 16/10 DEAE FF column in the anion exchange step and a HiPrep 16/10 Phenyl FF column for the hydrophobic interaction chromatography. Additionally, a final gel filtration step was introduced using a HiLoad Superdex 200 gel filtration column equilibrated with 10 mM HEPES, pH 7.5, 150 mM potassium chloride, and 4 mM dithiothreitol. Fractions containing YqjM were pooled and concentrated to 10 mg/ml by ultrafiltration using Centriprep-30 (Amicon). Selenomethionine-labeled YqjM (SeMet-YqjM) was expressed from the *met<sup>-</sup>* *Escherichia coli* strain B834(DE3). The purification of SeMet-YqjM followed the same protocol as for the native enzyme.

**Protein Crystallization**—Crystallization trials were performed at 19 °C using the sitting drop vapor diffusion method. After intensive screening, well diffracting crystals were obtained by mixing 3  $\mu$ l of

protein with 1.5  $\mu$ l of a crystallization solution containing 0.1 M Tris/HCl, pH 8.5, 25% polyethylene glycol 3500, and 0.2 M sodium chloride. Crystal trials were set up in cryschem plates with a reservoir volume of 400  $\mu$ l. After 5–7 days, crystal plates appeared that had the characteristic yellow color of the oxidized, enzyme-bound FMN cofactor. They belonged to the orthorhombic space group C222<sub>1</sub> with unit cell dimensions of  $a = 51.5$  Å,  $b = 185.2$  Å, and  $c = 169.8$  Å and contained two molecules per asymmetric unit corresponding to a solvent content of 54%. However the above-mentioned condition did not yield crystals of the SeMet-YqjM derivative. After a new screening round, a similar crystallization condition was found containing 0.1 M Tris/HCl, pH 8.5, 25% polyethylene glycol 3500, 0.2 M lithium sulfate, and 0.01 M strontium chloride. YqjM-SeMet crystals complexed with pHBA and pNP were obtained by cocrystallization using a ligand concentration of 3 mM. The presence of either pHBA or pNP resulted in a color change of the yellow YqjM crystals toward red. Reduction of YqjM crystals was achieved by soaking crystals of the oxidized enzyme in 100 mM NADPH until they turned colorless (approximately after 10 min). For cryomeasurements, crystals were transferred from the crystallization drop to the mother liquor supplied with 15% 2-methyl-2,4-pentanediol as cryo-protectant and rapidly frozen in a 100 K stream of nitrogen gas.

**Data Collection and Structure Determination**—Initial attempts to overcome the crystallographic phase problem by molecular replacement using several search models derived from other members of the OYE family failed. Therefore experimental phase information was required to determine the structure of YqjM. Phase information could be obtained by collecting a single-wavelength anomalous diffraction (SAD) data set from a single SeMet-YqjM crystal. SAD data of SeMet-YqjM and diffraction data of the complexes with pHBA and pNP were collected at the BW6 beamline at the Deutsches Elektronen Synchrotron (Hamburg, Germany) using a MarCCD detector. Crystals of the oxidized and reduced YqjM were measured in house using a MarResearch imaging plate.

All diffraction data were processed and scaled with the programs DENZO and SCALEPACK from the CCP4 package (18). For the SAD experiment, an x-ray absorption spectrum was recorded in the vicinity of the selenium edge. Diffraction data up to 1.8 Å resolution were then collected at a wavelength corresponding to the peak of this spectrum ( $f''$  maximum, 0.9792 Å). Subsequently, difference Fourier analyses performed with SHELX (19, 20) enabled us to identify all 10 of the theoretical selenium sites. Refinement of heavy atom parameters and phase calculation were conducted with SHARP (21) leading to a figure of merit of 0.68 for data between 20 and 1.82 Å resolution. Solvent flattening was performed with SOLOMON (22) and resulted in an electron density map of excellent quality, in which the entire backbone model of YqjM was built in with ARP/wARP (23). Energy-restrained crystallographic refinement against the 1.3 Å resolution data set was carried out with maximum likelihood algorithms implemented in CNS (24) using the protein parameters of Engh and Huber (25). Refinement, model rebuilding with the program O (26), and water incorporation proceeded smoothly via rigid body, positional, and later *B*-factor optimization. The entire structure was checked using simulated annealing composite omit maps. Finally, after the addition of the FMN cofactor molecules, the refinement converged at a *R*-factor of 18.9% ( $R_{\text{free}} = 20.8\%$ ). All residues of YqjM could be traced in the electron density map and exhibited good stereochemistry (Table I). Also the FMN cofactor molecules were well defined by electron density as well as four sulfate ions, two of which were bound within the active sites and the other two stabilizing crystal lattice contacts. In the Ramachandran plot, 91% of the 674 residues were found in the most favorable, 8.6% in the favorable, 0.3% in the generously allowed, and no residue was found in the disallowed region. The data collection, phasing, and refinement statistics are summarized in Table I. All parameter and topology files were created with the program XPLOR2D (27).

Graphical presentations were made using the programs MOLSCRIPT (28), RASTER3D (29), DINO (www.dino3d.org) and PYMOL (www.pymol.org).

**Sequence Alignment and Phylogenetic Reconstruction**—Amino acid sequences were retrieved by BLAST searches using the Swiss-Prot data base and aligned using the web-based program MULTALIN (available at [prodes.toulouse.inra.fr/multalin/multalin.html](http://prodes.toulouse.inra.fr/multalin/multalin.html)). To perform a phylogenetic analysis, the amino acid sequences were aligned with ClustalW and the result saved in the NEXUS format. The program PAUP\* 4.0b10 was used to analyze the phylogenetic relationships of the OYE/YqjM homologs.

**Enzyme Assays**—The apparent steady state kinetic constants were determined as described in Ref. 1. Briefly, the assays were performed in 0.1 M Tris/HCl, pH 7.5, at 25 °C in the presence of an oxygen-consuming

TABLE I  
 Crystallographic data collection and refinement statistics

	Oxidized YqjM	Reduced YqjM	YqjM/pHBA	YqjM/pNP
Data collection				
Unit cell	C222 <sub>1</sub>	C222 <sub>1</sub>	C222 <sub>1</sub>	C222 <sub>1</sub>
Cell constants (Å)	<i>a</i> = 51.5 <i>b</i> = 185.2 <i>c</i> = 169.8	<i>a</i> = 51.2 <i>b</i> = 184.6 <i>c</i> = 168.9	<i>a</i> = 51.2 <i>b</i> = 184.7 <i>c</i> = 169.2	<i>a</i> = 51.4 <i>b</i> = 184.8 <i>c</i> = 172.0
Resolution (Å) <sup>a</sup>	8–1.30 (1.32–1.30)	10–1.70 (1.73–1.70)	10–1.85 (1.88–1.85)	8–1.40 (1.42–1.40)
No. of unique reflections	183,799 (8068)	86,971 (4275)	66,570 (3211)	144,550 (7312)
Redundancy	2.35 (2.09)	2.96 (2.93)	2.71 (2.65)	2.82 (2.85)
Completeness (%)	92.7 (82.2)	99.0 (98.7)	97.3 (94.8)	96.3 (97.5)
<i>R</i> <sub>sym</sub> (%) <sup>b</sup>	4.3 (34.2)	3.3 (14.6)	8.5 (22.1)	7.5 (14.1)
<i>I</i> / $\sigma$ ( <i>I</i> )	20.6 (2.0)	26.5 (7.0)	16.6 (4.6)	18.2 (4.9)
Refinement				
<i>R</i> <sub>cryst</sub> / <i>R</i> <sub>free</sub> (%) <sup>c</sup>	18.9/20.8	17.9/19.9	18.2/20.4	19.6/21.2
No. of atoms (mean B (Å <sup>2</sup> ))				
Protein	5274 (18.3)	5274 (20.4)	5274 (15.0)	5274 (13.6)
FMN	62 (12.8)	62 (17.7)	62 (10.0)	62 (9.6)
Sulfate	20 (47.7)		10 (57.6)	10 (58.7)
Ligand			18 (15.5)	30 (23.8)
Water	842 (32.7)	669 (33.8)	622 (26.7)	642 (25.6)
r.m.s.d. bond length (Å)	0.014	0.006	0.005	0.006
r.m.s.d. bond angles (°)	1.55	1.28	1.28	1.29
r.m.s.d. <i>B</i> -factors (Å <sup>2</sup> )	2.13	2.28	2.22	2.19

<sup>a</sup> Values for the highest resolution shells are given in parentheses.

<sup>b</sup>  $R_{\text{sym}} = \frac{\sum_{hkl} \sum_j |I_j - \langle I \rangle|}{\sum_{hkl} \sum_j I_j(hkl)}$ , where  $\langle I \rangle$  is the mean intensity of reflection  $hkl$ .

<sup>c</sup>  $R_{\text{cryst}} = \frac{\sum_{hkl} |F_{\text{obs}} - F_{\text{calc}}|}{\sum_{hkl} |F_{\text{obs}}|}$ , where  $F_{\text{obs}}$  and  $F_{\text{calc}}$  are the observed and calculated structure factor amplitude for reflections  $hkl$  included in the refinement, respectively.  $R_{\text{free}}$  is the *R*-value for 5% of randomly selected reflections excluded from refinement.

system and followed by the oxidation of  $\beta$ -NADPH (100  $\mu$ M) at 340 nm in a Uvikon spectrophotometer while systematically varying the substrate concentration.

## RESULTS AND DISCUSSION

**Overall Structure**—The x-ray structure of native oxidized YqjM was solved by SAD and refined at 1.3 Å resolution to an *R*-factor of 18.9% (Table I). The monomer of YqjM is comprised of one compact domain representing the frequently observed ( $\alpha/\beta$ )<sub>8</sub>-barrel or TIM barrel fold, where a cylindrical core of eight twisted  $\beta$ -strands is surrounded by eight helices (Fig. 1). Similar to other ( $\alpha/\beta$ )<sub>8</sub>-structures, all of the turns at the NH<sub>2</sub>-terminal end of the barrel are composed of only three or four residues, while the loops at the COOH-terminal end are much longer and build up the active site. The numbering of these loops refers to the preceding  $\beta$ -strands, e.g. loop L6 follows strand 6 (see also Fig. 1B for nomenclature of secondary structure). The COOH-terminal loops range in length from 5 to 31 residues and harbor additional secondary structural elements, namely helices  $\alpha$ B,  $\alpha$ C,  $\alpha$ D, and  $\alpha$ E and strands  $\beta$ C and  $\beta$ D. In addition, YqjM has a  $3_{10}$ -helix  $\alpha$ A and two short antiparallel  $\beta$ -strands prior to  $\beta$ -strand 1 that close the barrel on its NH<sub>2</sub>-terminal side. A short  $3_{10}$ -helix  $\alpha$ F is present after the COOH-terminal helix 8.

The overall structure of YqjM strongly resembles the structures of other OYE homologs (13–17). The closest structural relative was found to be pentaerythritol tetranitrate (PETN) reductase from *Enterobacter cloacae* where 278 residues could be aligned with a root mean square deviation (r.m.s.d.) value of 1.29 Å, followed by morphinone reductase (MR) from *P. putida* (286 aligned C $\alpha$  with an r.m.s.d. of 1.41 Å), 12-oxophytodienoate reductase (OPR) 1 from *Lycopersicon esculentum* (286 C $\alpha$ , 1.46 Å) and OYE (282 C $\alpha$ , 1.48 Å). A common feature among these oxidoreductases is the NH<sub>2</sub>-terminal  $\beta$ -hairpin structure that lids the  $\beta$ -barrel. Except for the loops L4 and L8, all COOH-terminal loops of the  $\beta$ -barrel adopt conformations that are distinct in the OYE flavoproteins. In general, these loops form the active site and provide substrate as well as reaction specificity. While other members of the OYE family show some similarities in the respective loop structures, YqjM exhibits unique structural features in the corresponding active site

region. Especially the loops L3, L5, and L6 adopt different conformations and vary considerably in length. For example, the crystal structures of OPR1 (16), PETN reductase (15), and MR (14) have shown that the loop L3 forms a part of the hydrophobic active site tunnel and seems to play a role in substrate discrimination. In these enzymes loop L3 is extended and folds as an additional two stranded  $\beta$ -sheet, which covers half of the active site. In contrast, the corresponding loop of YqjM is folded as a short  $3_{10}$ -helix ( $\alpha$ C), which is packed on the wall of the  $\beta$ -barrel. As a result, the YqjM active site is hardly protected by any loop structure and thus is remarkably wide and accessible for potential substrate molecules.

**Oligomerization State and Oligomer Interfaces**—The oligomeric state of YqjM observed in the crystal is the same as in solution (11). It is a tetrameric enzyme, in which the subunits are organized with 222 (D2) point group symmetry (Fig. 2). The tetramer has overall dimensions of  $\sim 84 \times 92 \times 47$  Å<sup>3</sup> and resembles a four-petaled cloverleaf with a central hole. The subunits are arranged in such a way that their active sites, defined by the bound FMN molecule, open up in different directions to solvent but are connected with each other by the central hole. In the C222<sub>1</sub> crystal form, two of the 2-fold rotation axis coincide with the crystallographic *a* and *b* axis, respectively. The two monomers, which are present in the asymmetric unit (named A and B, their crystallographic symmetry mates C and D), are essentially identical and are related by a non-crystallographic 2-fold axis. As discussed below, the YqjM tetramer is organized as a dimer of active dimers, i.e. AB and CD, respectively. The ( $\alpha/\beta$ )<sub>8</sub>-domains of the corresponding monomers interact extensively around the dimer 2-fold axis such that their barrel axis are approximately parallel to each other but open up into opposite directions. The dimer axis passes between helix 1 of the two monomers, where both elements come close together. Additionally, interaction of helix  $\alpha$ E and the entire COOH terminus including helix  $\alpha$ F with the neighboring counterpart contribute considerably to the binding energy of both subunits. The interaction sites  $\alpha 1/\alpha 1^*$  and the  $\alpha F/\alpha F^*$  are arranged in a perpendicular fashion and are stabilized by the formation of a large hydrophobic cluster involving residues Met<sup>27</sup>, Pro<sup>39</sup>, Phe<sup>40</sup>, Met<sup>42</sup>, Ala<sup>43</sup>, Ile<sup>46</sup>, Ile<sup>50</sup>, Pro<sup>314</sup>,

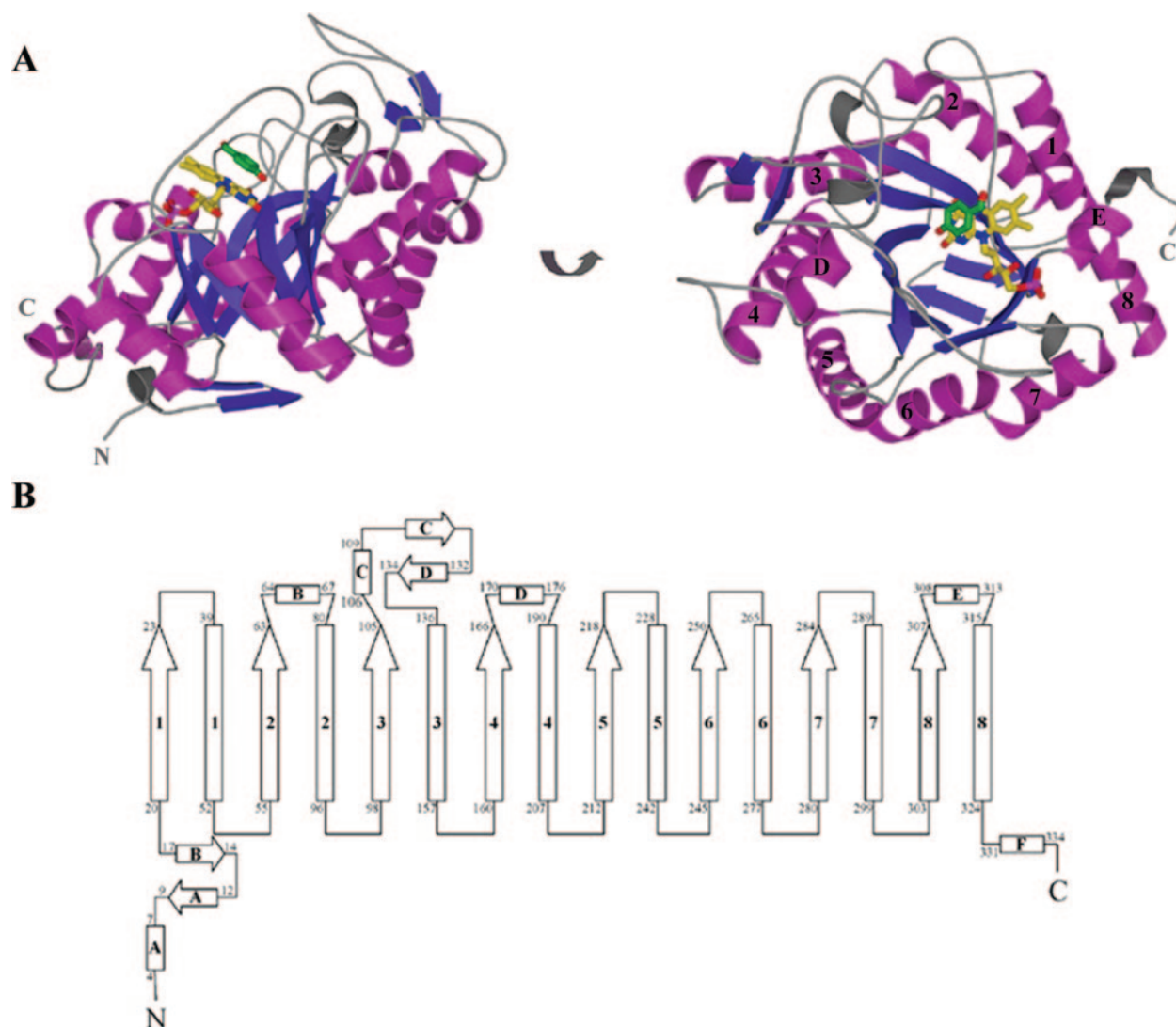


FIG. 1. *A*, ribbon diagram of the YqjM monomer complexed with pHBA in orthogonal mode. YqjM is colored according to its secondary structure: magenta, helices; violet,  $\beta$ -strands, and gray, coils. The flavin cofactor and the ligand pHBA are drawn in stick form with FMN in yellow and the ligand in green. *B*, topology of YqjM. Helices are displayed as rectangles and strands as arrows. The helices and strands of the barrel are numbered according to their order in the barrel. The extra barrel secondary elements are designated by letters. The numbers at the beginning and the end of each secondary element account for the amino acid number.

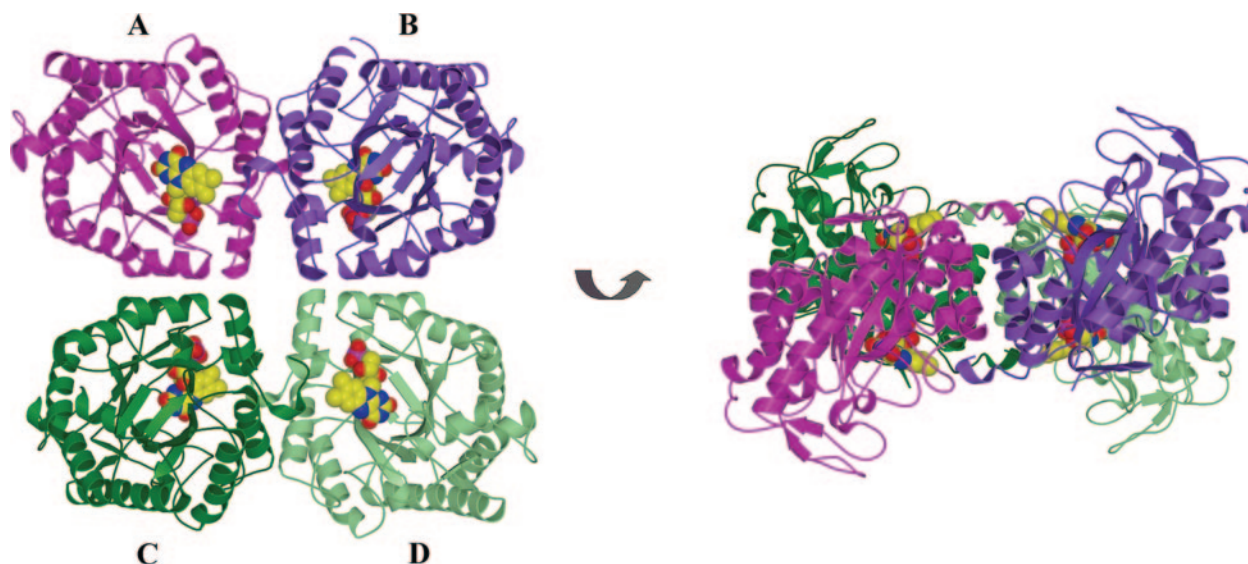


FIG. 2. **Ribbon diagram of the YqjM tetramer represented in orthogonal mode.** YqjM is a dimer of catalytically dependent dimers. Each subunit is colored differently. Functionally connected subunits are shown in similar colors. The cofactor FMN is presented in space filling form with carbon in yellow, oxygen in red, and nitrogen in blue.

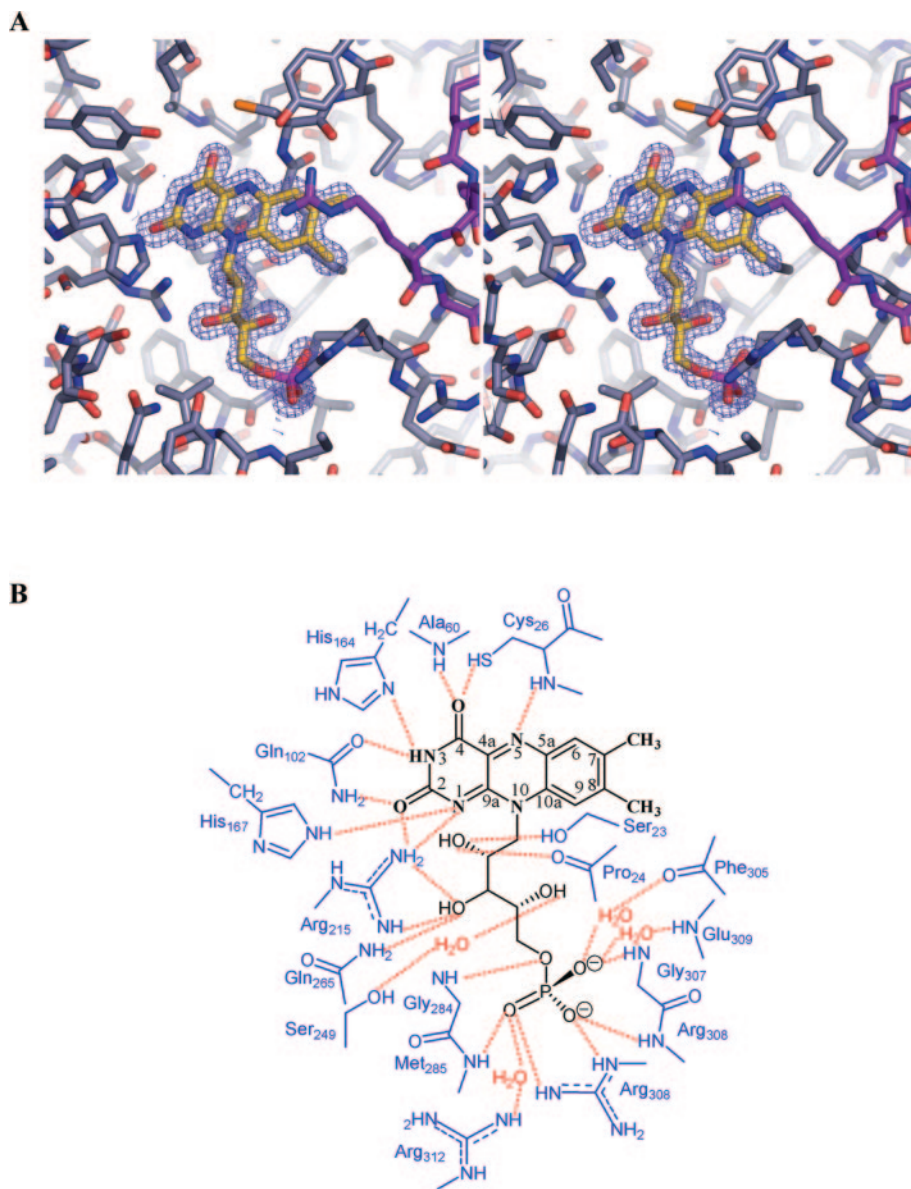


FIG. 3. **The flavin binding site.** *A*, stereo view of the flavin binding site. The final 1.3 Å resolution  $2F_o - F_c$  map is contoured at  $1.5\sigma$ . The flavin and the side chains of the amino acids are drawn in *ball-and-stick* mode, with FMN in *yellow* and the residues from monomer *A* in *gray* and from the neighboring monomer *B* in *violet*. *B*, schematic illustration of the interaction of FMN with active site residues. The *thin red dotted lines* illustrate hydrogen bonds.

and Phe<sup>315</sup>. This cluster is enclosed by a pronounced hydrogen bonding network formed by Ser<sup>29</sup>, His<sup>44</sup>, Arg<sup>48</sup>, Leu<sup>311</sup>, Arg<sup>312</sup>, Gln<sup>333</sup>, Tyr<sup>334</sup>, Arg<sup>336</sup>, Gly<sup>337</sup>, and Trp<sup>338</sup>. Most notably, the COOH-terminal end is directed by the latter interactions toward the active site of the neighboring subunit. One of the COOH-terminal residues Arg<sup>336\*</sup> (the asterisk denotes the neighboring subunit) is even protruding as an arginine finger into the adjacent active site, where it forms a part of the substrate binding pocket (near the flavin dimethyl benzene ring). Thus the shared active site strongly suggests that the dimer is the active unit of YqjM. Its formation shields 1241 Å<sup>2</sup> per monomer (9% of the entire monomer surface), while the other monomer-monomer contacts are considerably smaller. The contact area between *A* and *C* comprises 5% of the accessible monomer surface and the monomers *A* and *D* do not interact at all with each other. The contacts between the dimers *AB* and *CD* are mediated by the helix-loop-helix motifs of helices 6 and 7 and comprise mainly hydrophobic interactions involving Val<sup>260</sup>, Phe<sup>261</sup>, Pro<sup>262</sup>, Tyr<sup>264</sup>, Val<sup>266</sup>, Met<sup>285</sup>, and Met<sup>291</sup>. The few polar interactions are established by Gly<sup>263</sup>, Glu<sup>270</sup>, Asn<sup>298</sup>, Arg<sup>300</sup>, and their symmetry mates.

As mentioned earlier, YqjM is the only known tetrameric enzyme of the OYE family identified so far. While OPR and MR

exist as monomers, OYE (13) as well as MR (14) were found to be dimeric enzymes. An important difference in YqjM compared with OYE and MR is the shared active site with the contribution of the COOH-terminal Arg<sup>336\*</sup> of the neighboring subunit. In the related MR, the COOH terminus forms similar secondary structural elements as in YqjM, which however, fold back onto their own subunit. Also the observed dimers of OYE and MR are formed by entirely different interfaces involving helices 4, 5, and 6 in OYE and helices 2, 8, and the NH<sub>2</sub>-terminal  $\beta$ -strands in MR. In both cases, the dimer subunits function as independent entities.

The structural data also explain earlier observations that a COOH-terminal hexahistidine tag disrupts the quaternary assembly leading to the formation of monomeric and dimeric enzyme forms (11). Since the structural data show that the COOH terminus of native YqjM contributes considerably to the close interaction with the neighboring subunit, a COOH-terminal extension impairs the formation of the *AB* dimer and also critically interferes with substrate binding and subsequently catalysis (11).

**The Flavon Binding Site**—YqjM binds the FMN cofactor non-covalently at the carboxyl-terminal end of the  $\beta$ -barrel, particularly above the  $\beta$ -strands 1 and 8. The isoalloxazine ring

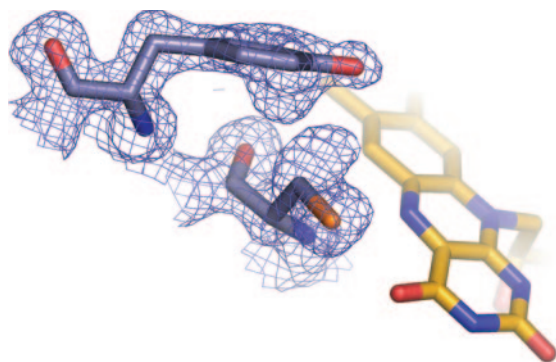


FIG. 4. **Electron density map of Cys<sup>26</sup> and Tyr<sup>28</sup> in the active site.** The  $3F_o - 2F_c$  map is contoured at  $1.2\sigma$ . Amino acids and FMN are presented as in Fig. 3.

occupies a similar orientation as in other OYEs with its *re*-side facing the protein and its *si*-side directed to solvent (Fig. 3).

In contrast to OPR and MR, where the isoalloxazine ring is planar (14, 16), the electron density for the oxidized FMN cofactor in YqjM revealed unequivocally the so-called butterfly bending at the hypothetical N(5)-N(10) hinge. This result is surprising since the oxidized flavin ring system is widely described to be planar (30–32). It was assumed that only upon reduction the isoalloxazine molecule bends along the N(5)-N(10) axis. However, reduction of YqjM does not lead to any further bending of the isoalloxazine ring. The observed deviation from planarity for the YqjM flavin might be a result of interactions with the apoprotein in such a way that could modulate its chemical behavior.

In fact, the redox chemistry of the flavin is controlled and precisely tuned by several interactions with the apoprotein as illustrated in Fig. 3. Many of these interactions are conserved within the OYE family. In the following we will describe similarities and differences in binding the FMN cofactor starting with the isoalloxazine ring and moving then to the ribityl side chain and the terminal phosphate group.

Similarly as in OYE, the specific electronic contribution of the pyrimidine ring is determined by interactions of a glutamine (Gln<sup>102</sup>) with N(3) and O(2) as well as of an arginine (Arg<sup>215</sup>) with O(2) and N(1). Furthermore, N(1) is hydrogen bonded to His<sup>167</sup> and N(3) to His<sup>164</sup>. The FMN O(4) is in hydrogen bonding distance to the main chain carbonyl oxygen of Ala<sup>60</sup> and the Cys<sup>26</sup> sulfhydryl group. Also comparable with OYE, in YqjM, the dimethyl benzene ring of FMN is bound to the protein by hydrophobic interactions with the side chains of Met<sup>25</sup>, Leu<sup>311</sup>, and Arg<sup>308</sup>. In contrast, the whole lateral part of the flavin binding pocket is strikingly differently organized (Fig. 3A). Notably, instead of a bulky aromatic phenylalanine as in all other OYE homologs, an arginine (Arg<sup>336\*</sup>) protrudes from the neighboring monomer and forms part of the flavin binding pocket (Fig. 3A).

The ribityl moiety of the cofactor is anchored to Arg<sup>215</sup>, Ser<sup>23</sup>, Ser<sup>249</sup>, Gln<sup>265</sup>, and the main-chain atom of Pro<sup>24</sup>. Furthermore, the proline main chain carbonyl oxygen is equidistant to N(1) and N(5) and may play a role in stabilizing the reduced flavin. Like the other OYE enzymes, the FMN phosphate group is embedded in an electropositive groove of the apoprotein that is formed by loops L7 and L8. Here, the positively charged guanidino group of Arg<sup>308</sup> and the main chain atoms of Gly<sup>284</sup>, Met<sup>285</sup>, Phe<sup>305</sup>, Gly<sup>307</sup>, Arg<sup>308</sup>, and Glu<sup>309</sup> are involved in an extensive network of polar interactions with the phosphate group and thereby enable FAD and FMN to be discriminated between. The FMN phosphate is bound further by the positive end of the macro dipole of helix  $\alpha$ E and by the guanidino group of Arg<sup>312</sup> that is involved in a strong, water-mediated interac-

tion. Remarkably, the phosphate recognition motif of YqjM seems to be unique and is not shared by any other member of the OYE family.

Another difference to other OYE structures is that O(4) is not hydrogen-bonded to the side chain of a threonine, which has been shown to control the redox potential of the FMN cofactor in OYE (12). Instead, it interacts with Cys<sup>26</sup> (Fig. 3B). Moreover, the electron density map of the free enzyme shows clearly that this cysteine can adopt several conformations (Fig. 4). It either interacts with the flavin O(4) or alternatively forms a hydrogen bond with N(5), indicating that the redox properties of the flavin might be altered depending on the conformation of Cys<sup>26</sup>. Furthermore, the side chain of Cys<sup>26</sup> has the ability to interact with the delocalized ring electrons of Tyr<sup>28</sup> (Fig. 4). Interestingly, in the presence of each of the ligands (pHBA or pNP), Cys<sup>26</sup> points exclusively toward O(4) (Fig. 5). These observations may suggest that Cys<sup>26</sup> might act as a redox sensor that controls the redox potential of flavin depending on the presence of substrates. Future studies will aim at testing this hypothesis.

**The Substrate Binding Site**—The major difference in YqjM compared with related OYE enzymes is manifested in the construction of the substrate binding pocket. Our structural analyses of the oxidized and the reduced enzyme, and of complexes with various ligands, provide valuable insight into how substrate selection might be achieved. The ligands chosen in this analysis were pHBA and pNP, which are phenolic aromatic compounds acting as competitive substrate inhibitors.

The  $F_o - F_c$  electron density map of the uncomplexed oxidized enzyme shows a strong positive peak above the flavin isoalloxazine ring, which is most probably caused by a bound sulfate ion, a component of the crystallization solution (Fig. 5). A similar observation was reported for OYE (13) and PETN reductase (15). In both cases, a chloride ion occupies the corresponding position in the active site. The sulfate ion was bound specifically by Tyr<sup>28</sup>, Lys<sup>109</sup>, His<sup>164</sup>, His<sup>167</sup>, Tyr<sup>169</sup>, and Arg<sup>336\*</sup> and might point to some characteristics of the physiological substrate. In accordance with the structural data obtained for OYE and PETN reductase, the reduction of oxidized YqjM crystals with NADPH resulted in the replacement of the sulfate ion by two water molecules, thus reflecting the changed electronic state of the flavin dihydroquinone.

Fitzpatrick *et al.* (1) have shown that phenolic inhibitors bind in the anionic phenolate state, which is in agreement with the architecture of the active site. Similar to OYE, the ligand phenolic group is located within hydrogen bonding distance to His<sup>164</sup> and His<sup>167</sup>, whereas the aldehyde group of pHBA is bound via the hydroxyl group of Tyr<sup>28</sup> thereby aligning the compound parallel above the *si*-face of the flavin cofactor (Fig. 5). Proper positioning of pNP in the active site requires an additional hydrogen bond between the nitro group and Arg<sup>336\*</sup> from the neighboring subunit above the flavin xylene ring (Fig. 5). The before mentioned Lys<sup>109</sup> that is involved in the binding of the sulfate has no function in binding either of the ligands.

While the binding of the proximal anionic hydroxyl group of various ligands in YqjM via the two histidines His<sup>164</sup> and His<sup>167</sup> equals the binding motifs of other OYE homologs (His<sup>191</sup> and Asn<sup>194</sup> in OYE (13), His<sup>187</sup> and His<sup>190</sup> in OPR1 (16), His<sup>186</sup> and Asn<sup>189</sup> in MR (14), and His<sup>181</sup> and His<sup>184</sup> in PETN reductase (15)), there are striking differences in binding the distal functional group of the inhibitors. For example, a tyrosine residue generally serves as the binding partner for the aldehyde as well as the nitro group of the characterized inhibitors (Fig. 5). However, the OYE tyrosine originates from a COOH-terminal fragment (Tyr<sup>375</sup>), whereas in YqjM the NH<sub>2</sub>-terminal Tyr<sup>28</sup> is involved. Apparently, to bind a substrate, a tyrosine

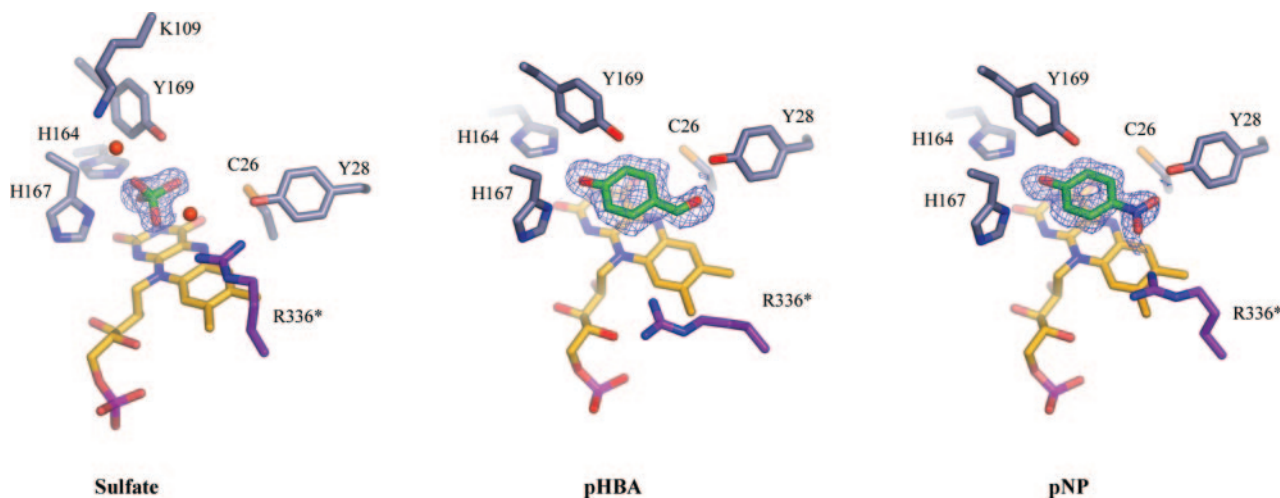


FIG. 5. **The substrate binding site.** All residues are displayed in *ball-and-stick* mode with the flavin in *yellow* and the ligands (sulfate, pHBA, pNP) in *green*. Water molecules are represented as *red spheres*. Side chains of selected active site residues of monomer A are displayed in *gray* and from monomer B in *violet*. The  $2F_o - F_c$  density maps for the ligands are contoured at  $1\sigma$ .

A	YqjM	20	IVMSPPCMYSSHEKDGKLT <sup>◆</sup> PFHMAHYISRAI	50
	Consensus		I..sPMCnys....dG.andwH.vHygsra.	
	ScOYE3	31	AVMPPLTRMRATHP	44
	Consensus		.v.aP.TR.Ra...	
B	YqjM	162	EIHAAHGYLI	171
	Consensus		EIHaaHGyLl	
	ScOYE3	189	EIHSANGYLL	198
	Consensus		Eih.angyLl	
C	YqjM	310	LLRDPFFARTAAKQLNTEIPAPVQYERGW	338 (338)
	Consensus		lLRdPywp..Aa..Lg.....P.QY.RA.	
	ScOYE3	373	TFYTMSAEGYTDYPT <sup>▽</sup> YEE	390 (399)
	Consensus		tfY.....GYtdypf..e	

FIG. 6. **Partial sequence alignments.** Shown are segments of the YqjM amino acid sequence (*first line*) and of OYE3 from *S. cerevisiae* (*third line*). Below are the consensus sequences obtained from an alignment of 12 members of the YqjM and OYE family, respectively (see also legend to Fig. 7). *Capital letters* indicate 90% conservation, while *lowercase letters* indicate conservation in more than 50% of the sequences. *Numbers* indicate the position of the first and last amino acid shown in the alignment. The *arrows* in A and C designate the invariant amino acids involved in the dimerization interface of YqjM (His<sup>44</sup>, Arg<sup>48</sup> in A and Arg<sup>312</sup>, Gln<sup>333</sup>, Tyr<sup>334</sup>, and Arg<sup>336</sup> in C). The *diamonds* in A mark the position of Cys<sup>26</sup> in YqjM and Thr<sup>37</sup> in OYE3, respectively. *Asterisks* in B denote the amino acids that are conserved in the active site of both YqjM and OYE (His<sup>164</sup> and His<sup>191</sup> in YqjM and OYE3, respectively; His<sup>167</sup> and Asn<sup>194</sup> in YqjM and OYE3, respectively; Tyr<sup>169</sup> and Tyr<sup>196</sup> in YqjM and OYE3, respectively). The *triangles* in A and C mark the tyrosine residue involved in binding of the phenolic ligand (Tyr<sup>28</sup> and Tyr<sup>375</sup> in YqjM and OYE3, respectively). *Numbers in parentheses* in C give the total number of amino acids in the respective proteins.

seemed to be evolutionary favored in all so far known OYEs, including YqjM, but interestingly in YqjM this residue is provided by a completely different structural part of the enzyme namely the loop region after strand  $\beta_1$  (L1). Intriguingly, this tyrosine in YqjM seems to be properly positioned by Cys<sup>26</sup>, one of the residues modulating the cofactor redox state.

As mentioned previously, a unique feature of YqjM is the shared active site that is partially formed by the COOH terminus of the neighboring subunit. The complex structure with pNP indicates that Arg<sup>336\*</sup> is directly involved in substrate/inhibitor recognition as it develops a strong hydrogen bond with the nitro group. Since this feature has not been observed in any other OYE homologs, the distinct YqjM active site ar-

chitecture might allow recruitment of a distinct substrate. Future studies are aimed to further characterize an optimal YqjM substrate, which should be instrumental in revealing the biological function of YqjM.

Comparison of the ligand complexes of YqjM and OYE (13) with pHBA demonstrates that the aromatic ring of the inhibitor is positioned in a similar parallel fashion to the flavin isoalloxazine ring, but in YqjM the aldehyde oxygen is rotated by 180° pointing in the opposite direction. This difference can be attributed to significant structural rearrangements in this part of the YqjM active center, in particular in the recruitment of Tyr<sup>28</sup> for the ligand binding.

However, in each case, pHBA as well as pNP is perfectly

aligned for the hydride transfer from the flavin N(5), although neither are substrates of YqjM. Furthermore, Tyr<sup>169</sup>, which is located 3.4 Å above the C(1) atom of pHBA and pNP (Fig. 5), can be considered as an acid catalyst protonating the substrate at the C(1) position in the oxidative half-reaction. This tyrosine residue superimposes perfectly with Tyr<sup>196</sup> in OYE (13), Tyr<sup>192</sup> in OPR (16), and Tyr<sup>186</sup> in PETN reductase (15). It has been shown that replacing Tyr<sup>196</sup> in OYE by a phenylalanine resulted in a dramatic slowing of the oxidative half-reaction with 2-cyclohexenone (33). Thus, a common catalytic mechanism can be anticipated for OYE, OPR, PETN reductase, and YqjM.

The backbone r.m.s.d values between free YqjM and the two complex structures are rather low (674 C $\alpha$ , 0.141 Å for pHBA, 674 C $\alpha$ , 0.163 Å for pNP) indicating that ligand binding does not induce pronounced structural rearrangements, not even in the active site. Only subtle but significant differences could be observed that are necessary to accommodate the ligands. In particular, the side chains of Tyr<sup>28</sup> and Arg<sup>336\*</sup> reorient to form proper hydrogen bonds. However, while Tyr<sup>28</sup> shifts only slightly away after binding of both ligands, Arg<sup>336\*</sup> rearranges markedly. Arg<sup>336\*</sup> can obviously adopt various conformations depending on the presence/absence of substrates/inhibitors (Fig. 5). In the uncomplexed, reduced enzyme, the side chain of Arg<sup>336\*</sup>, which was not involved in any specific contacts, was poorly defined by electron density. This indicates that it is highly flexible. In the uncomplexed, oxidized enzyme, a sulfate ion was bound in the active site with Arg<sup>336\*</sup> contributing to its coordination via interaction with an ordered water molecule resulting in one distinct, well defined conformation. In the presence of pNP, the side chain of Arg<sup>336\*</sup> adopts two distinct conformations, both of which support binding of the nitro group of the ligand. These findings illustrate how a flexible, single residue can support binding of different ligand molecules.

**Evidence for a New Class of OYE Oxidoreductases**—Similar sequences to those of *S. cerevisiae* OYE3 and *B. subtilis* YqjM were searched for in the Swiss-Prot data base. From each search, a total of 12 sequences were selected and aligned using MULTALIN. Inspection of the alignment revealed that the structural differences between OYE and YqjM noted before are also reflected by the conservation of different residues in these two groups of proteins. Most notably, Cys<sup>26</sup> and Tyr<sup>28</sup> are highly conserved in all YqjM family members, whereas all classical OYE homologs feature a highly conserved threonine in the equivalent position of Cys<sup>26</sup> (Fig. 6A). The conserved Tyr<sup>28</sup> in the YqjM family members has no equivalent in the classical OYE family, as this residue is replaced by Tyr<sup>375</sup> (OYE) in the active site of the enzyme. Hence, this residue is invariant in this family of enzymes. Another salient distinction is the highly conserved COOH terminus in the YqjM family, in particular the invariant Arg<sup>312</sup>, Gln<sup>333</sup>, Tyr<sup>334</sup>, and Arg<sup>336\*</sup> (Fig. 6C). The latter amino acid is involved in setting up the active site of the other monomer in the dimer (see also Fig. 5), and thus we predict that this contribution to the active site in the dimer is a conserved feature in the YqjM family. On the other hand, Arg<sup>312</sup> is involved in the flavin phosphate binding. Additionally, it participates together with Gln<sup>333</sup> and Tyr<sup>334</sup> in the formation of the characteristic dimer interface. Therefore these residues are only conserved in the YqjM but not in the OYE family. Likewise, other residues contributing to the dimer interface, such as His<sup>44</sup> and Arg<sup>48</sup>, are only conserved in the YqjM family (Fig. 6A). Based on this sequence analysis, it is evident that the structural characteristics of YqjM must also be present in other homologous proteins. Clearly, this family of YqjM homologs is distinct from the classical OYE homologs.

This conclusion is also supported by a phylogenetic analysis using sequences of both the OYE and YqjM family. As

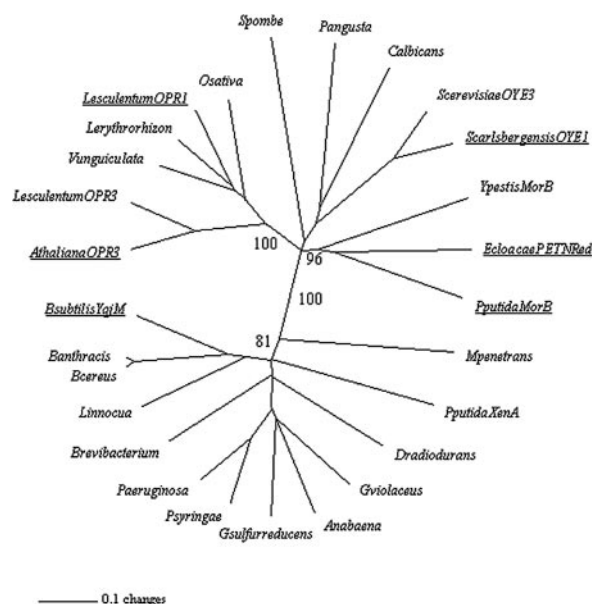


**FIG. 7. Phylogenetic reconstruction.** The unrooted phylogenetic tree was generated by neighbor joining. Numbers at the branches indicate the support from one thousand bootstrap runs (in percent). *Anabaena*, *Anabaena* sp.; *Athaliana*OPR3, *Arabidopsis thaliana* (oxophytodienoate reductase 3); *Banthracis*, *Bacillus anthracis*; *Bcereus*, *Bacillus cereus*; *Bsubtilis*YqjM, *B. subtilis* (YqjM); *Brevibacterium*, *Brevibacterium* sp.; *Calbicans*, *Candida albicans*; *Dradiodurans*, *Deinococcus radiodurans*; *Ecloacae*PETNRed, *E. cloacae* (pentaerythritol tetranitrate reductase); *Gsulfurreducens*, *Geobacter sulfurreducens*; *Gviolaceus*, *Gloeobacter violaceus*; *Linnocua*, *Listeria innocua*; *Lerythrorhizon*, *Lithospermum erythrorhizon*; *Lesculentum*OPR1 and OPR3, *L. esculentum* (oxophytodienoate reductase 1 and 3, respectively); *Mpenetrans*, *Mycoplasma penetrans*; *Osativa*, *Oryza sativa*; *Pangusta*, *Pichia angusta*; *Paeruginosa*, *Pseudomonas aeruginosa*; *Pputida*MorB, *P. putida* (morphinone reductase B); *Pputida*XenA, *P. putida* (xenobiotic reductase); *Psyringae*, *Pseudomonas syringae*; *Spombe*, *Schizosaccharomyces pombe*; *Scarlbergensis*OYE1, *S. carlsbergensis* (OYE1); *Scerevisiae*OYE3, *S. cerevisiae* (OYE3); *Vunguiculata*, *Vinca unguiculata*; *Ypestis*MorB, *Yersinia pestis* (morphinone reductase B). The species from which structures of OYE homologs were determined are underlined.

shown in Fig. 7, the proteins form two distinct clades, one comprising all of the classical OYE homologs (upper clade) and the other all of the YqjM homologs (bottom clade). The support for this tree, as evaluated by the bootstrap procedure implemented in PAUP, is very high, especially for the branch separating the two clades. Therefore, it can be concluded that YqjM is the first member of a subfamily of OYE homologs that so far only comprises bacterial proteins, whereas the classical OYE family possesses members of both prokaryotic and eukaryotic (yeast and plants) species.

The conservation pattern of the newly discovered YqjM family and the classical OYE family was plotted onto the surface of both enzymes (Fig. 8, A and B) and manifested once more the so far described differences of both families. As expected, residues that are involved in the dimer or tetramer formation are highly conserved in YqjM and differ from OYE. While residues forming the flavin binding pocket are in the OYE and the YqjM family similarly highly conserved, residues determining the probable substrate binding site exhibit considerable different patterns. Moreover, in addition to the previously described residues in YqjM (Tyr<sup>28</sup>, His<sup>164</sup>, His<sup>167</sup>, and Arg<sup>336\*</sup>), Lys<sup>109</sup>, which is situated at the distant entrance of the active site, is conserved within the whole YqjM family and, therefore, is suggested to function in substrate binding. The neighboring Arg<sup>108</sup> as well as His<sup>105</sup> are also conserved. However, they seem to play a role in adjusting the active site rather than direct substrate binding. Another

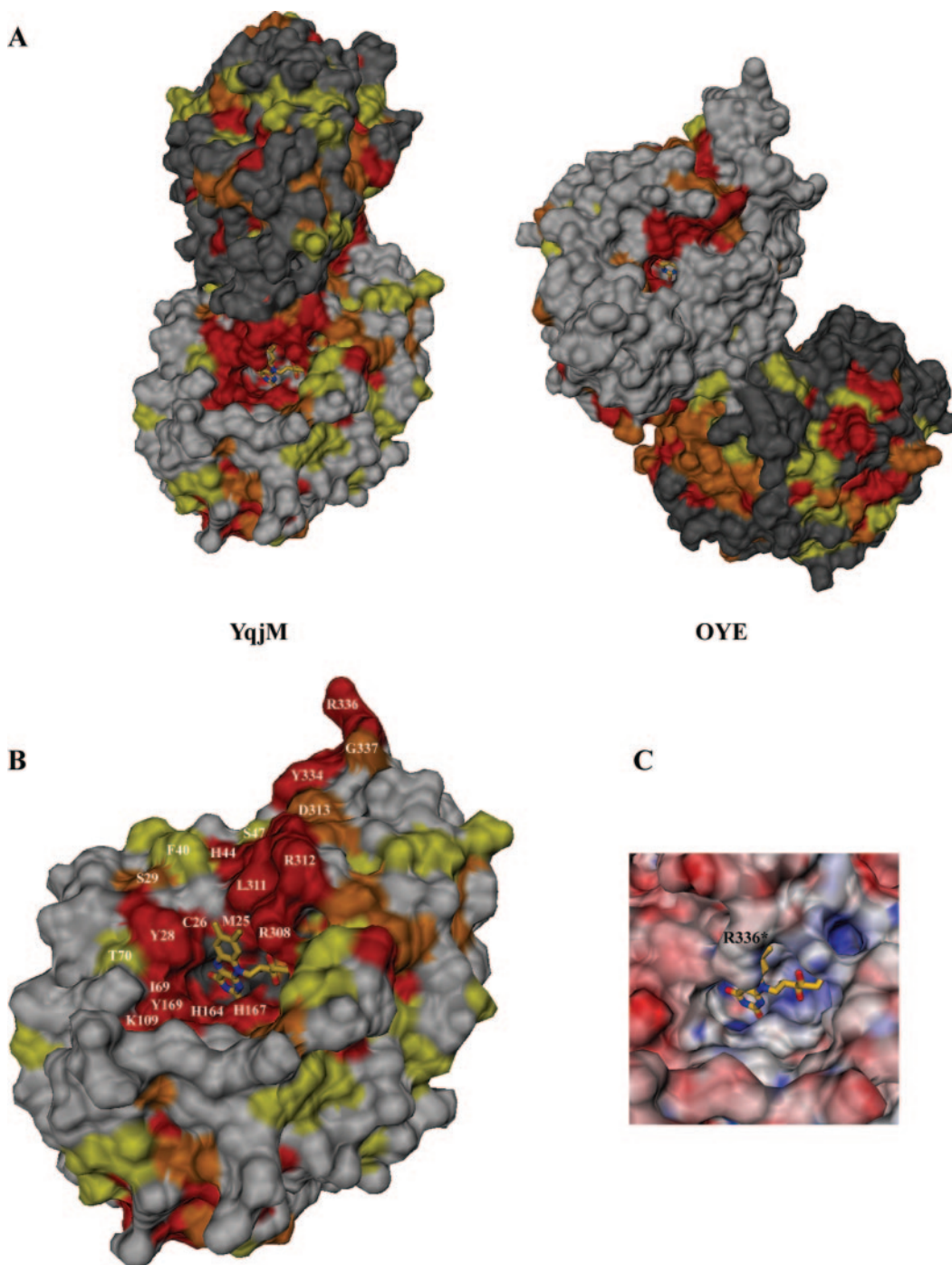


FIG. 8. **Surface properties of YqjM.** Conserved residues obtained from the sequence alignment of the YqjM and the OYE families (see Figs. 6 and 7) are mapped on the respective surfaces (A, YqjM and OYE dimer; B, YqjM monomer). Red indicates the strictly conserved residues. The degree of conservation is decreasing from red (more than 90%) over orange (more than 75%) to yellow (more than 50%). The electrostatic potential in the active site was mapped onto the surface of YqjM (C). Red indicates negatively charged and blue positively charged areas.

residue, whose strict conservation and proximity to the flavin cofactor indicates a role in substrate binding, is Thr<sup>70</sup>. The nearby conserved Asp<sup>73</sup> is situated within hydrogen bonding distance to Tyr<sup>28</sup>. The active site access above the flavin is determined by hydrophobic residues namely Ile<sup>69</sup> and Phe<sup>124</sup>, both of which are conserved within the family. Apart from His<sup>164</sup>, His<sup>167</sup>, and Tyr<sup>169</sup>, none of the residues mentioned here show conservation in the OYE family, thus indicating significant differences in the substrate specificity. Assuming that OYE as well as YqjM derives from a common ancestor, a divergent evolution must have occurred that adapted YqjM to its specific function and a specific substrate.

*Implications toward the Natural Substrate*—The architecture of the active site of YqjM in combination with steady state kinetic investigations provides information toward the true nature of the substrate of this enzyme. Activity assays were performed with duroquinone, menadione, prednisone, and 1,4-androstadiene 3,17-dione and compared with the kinetic data obtained for cyclohex-2-enone and *trans*-hex-2-enal published in Ref. 1 (Table II). The turnover rates with cyclohex-2-enone, duroquinone, menadione, and *trans*-hex-2-enal are very similar, while no NADPH oxidation could be observed with 1,4-androstadiene 3,17-dione or prednisone. This indicates that the active site can accommodate at least two ring systems but not

TABLE II  
Steady state kinetic data of YqjM

Substrate	$k_{\text{cat}}$ $\text{s}^{-1}$	$K_m$ $\mu\text{M}$	$k_{\text{cat}}/K_m$ $\mu\text{M}^{-1}\cdot\text{s}^{-1}$
Cyclohex-2-enone <sup>a</sup>	4.38	293 ± 29	0.0150
<i>trans</i> -Hex-2-enal <sup>a</sup>	4.68	2602 ± 186	0.0018
Duroquinone	2.67	19 ± 0.8	0.141
Menadione	3.04	≥841 ± 139	≤0.0036
Prednisone	ND <sup>b</sup>	ND <sup>b</sup>	ND <sup>b</sup>
1,4-Androstadiene 3,17-dione	ND <sup>b</sup>	ND <sup>b</sup>	ND <sup>b</sup>

<sup>a</sup> Taken from Ref. 1.

<sup>b</sup> ND, not detectable.

four. However, specificity appears to be introduced by the presence of the carbonyl functional group, with duroquinone, which has two carbonyl groups showing the highest specificity ( $k_{\text{cat}}/K_m$  0.141  $\mu\text{M}^{-1}\cdot\text{s}^{-1}$ ). The specificity also indicates the preference for a single ring system and could even be taken to imply that the enzyme prefers substrates with a second functional group opposite to the first. Thus, the kinetic data confirm our structural prediction that the unique construction of the YqjM active site points to the presence of a second binding site for a functional group that is defined by the residues Tyr<sup>28</sup> and Arg<sup>336\*</sup>. This group has to be partially electronegative and should be located opposite to the carbonyl function as is the case for several quinones, *e.g.* ubiquinone. Since the active site pocket is very hydrophobic (Fig. 8C) and based on the activity with *trans*-hex-2-enal, it would also be conceivable that the physiological substrate could incorporate one or more aliphatic side chains containing functional groups. Further anchoring points seem to be represented by Lys<sup>109</sup> and Thr<sup>70</sup>.

Fig. 8 clearly illustrates that the YqjM active site is wide open, easily accessible, and hydrophobic. Together with the present kinetic data, this construction argues against the adaptation toward a specific substrate molecule. It rather appears that the huge substrate binding pocket guarantees binding of a large spectrum of different substrate molecules allowing the transfer of redox equivalents from NADPH to a bunch of suitable oxidants, as proposed previously (1). Such an unspecificity would be essential to control the net redox state of the cell which might be disturbed by oxidative stress. Alternatively, the large hydrophobic flavin pocket of YqjM might be required to accept another protein as substrate. Future work is anticipated to determine the physiological substrate(s) of YqjM and clarify whether it is a protein or a small molecular weight compound.

**Acknowledgments**—We thank the staff of BW6 beamline at the Deutsches Elektronen Synchrotron in Hamburg for their assistance and Ruth Willmott for critical reading of the manuscript.

## REFERENCES

1. Fitzpatrick, T. B., Amrhein, N., and Macheroux, P. (2003) *J. Biol. Chem.* **278**, 19891–19897
2. Warburg, O., and Christian, W. (1932) *Naturwissenschaften* **20**, 688
3. Theorell, H. (1935) *Biochem. Z.* **275**, 344–346
4. Theorell, H., and Nygaard, A. P. (1954) *Arkiv. Kemi* **7**, 205–209
5. Theorell, H., and Nygaard, A. P. (1954) *Acta Chem. Scand.* **8**, 1104–1105
6. Abramovitz, A. S., and Massey, V. (1976) *J. Biol. Chem.* **251**, 5327–5336
7. Massey, V., and Schopfer, L. M. (1986) *J. Biol. Chem.* **261**, 1215–1222
8. Stott, K., Saito, K., Thiele, D. J., and Massey, V. (1993) *J. Biol. Chem.* **268**, 6097–6106
9. Vaz, A. D. N., Chakraborty, S., and Massey, V. (1995) *Biochemistry* **34**, 4246–4256
10. Haarer, B. K., and Amberg, D. C. (2004) *Mol. Biol. Cell* **15**, 4522–4531
11. Fitzpatrick, T. B., Auweter, S., Kitzing, K., Clausen, T., Amrhein, N., and Macheroux, P. (2004) *Protein Expression Purif.* **36**, 280–291
12. Xu, D., Kohli, R. M., and Massey, V. (1999) *Proc. Natl. Acad. Sci. U. S. A.* **96**, 3556–3561
13. Fox, K. M., and Karplus, P. A. (1994) *Structure* **2**, 1089–1105
14. Barna, T., Messiha, H. L., Petosa, C., Bruce, N. C., Scrutton, N. S., and Moody, P. C. E. (2002) *J. Biol. Chem.* **277**, 30976–30983
15. Barna, T. M., Khan, H., Bruce, N. C., Barsukov, I., Scrutton, N. S., and Moody, P. C. E. (2001) *J. Mol. Biol.* **310**, 433–447
16. Breithaupt, C., Strassner, J., Breiting, U., Huber, R., Macheroux, P., Schaller, A., and Clausen, T. (2001) *Structure* **9**, 419–429
17. Malone, T. E., Madson, S. E., Wrobel, R. L., Jeon, W. B., Rosenberg, N. S., Johnson, K. A., Bingman, C. A., Smith, D. W., Phillips, G. N., Jr., Markley, J. L., and Fox, B. G. (2005) *Proteins* **58**, 243–245
18. Bailey, S. (1994) *Acta Crystallogr. Sect. D Biol. Crystallogr.* **50**, 760–763
19. Sheldrick, G. M., and Schneider, T. R. (1997) in *Macromolecular Crystallography*, Part B, Vol. 277, pp. 319–343
20. Sheldrick, G. M. (2002) *Z. Kristallogr.* **217**, 644–650
21. de La Fortelle, E., and Bricogne, G. (1997) in *Macromolecular Crystallography*, Part A (Carter, Jr., C. W., and Sweet, R. M., eds) Vol. 276, pp. 472–494, Academic Press, New York
22. Abrahams, J. P., and Leslie, A. G. W. (1996) *Acta Crystallogr. Sect. D Biol. Crystallogr.* **52**, 30–42
23. Perrakis, A., Morris, R., and Lamzin, V. S. (1999) *Nat. Struct. Biol.* **6**, 458–463
24. Brünger, A. T., Adams, P. D., Clore, G. M., L., D. W., Gros, P., Grosse-Kunstleve, R. W., Jiang, J. S., Kuszewski, J., Nilges, M., Pannu, Read, R. J., Rice, L. M., Simonson, T., and Warren, G. L. (1998) *Acta Crystallogr. Sect. D Biol. Crystallogr.* **54**, 905–921
25. Engh, R. A., and Huber, R. (1991) *Acta Crystallogr. Sect. A* **47**, 392–400
26. Jones, T. A., Zou, J. Y., Cowan, S. W., and Kjeldgaard, M. (1991) *Acta Crystallogr. Sect. A* **47**, 110–119
27. Kleywegt, G., and Jones, T. (1998) *Acta Crystallogr. Sect. D Biol. Crystallogr.* **54**, 1119–1131
28. Kraulis, P. J. (1991) *J. Appl. Crystallogr.* **24**, 946–950
29. Merritt, E. A., and Murphy, M. E. P. (1994) *Acta Crystallogr. Sect. D Biol. Crystallogr.* **50**, 869–873
30. Hasford, J. J., Kemnitz, W., and Rizzo, C. J. (1997) *J. Org. Chem.* **62**, 5244–5245
31. Simonsen, R. P., and Tollin, G. (1980) *Mol. Cell. Biochem.* **33**, 13–24
32. Massey, V., Muller, F., Feldberg, R., Schuman, M., Sullivan, P. A., Howell, L. G., Mayhew, S. G., Matthews, R. G., and Foust, G. P. (1969) *J. Biol. Chem.* **244**, 3999–4006
33. Kohli, R. M., and Massey, V. (1998) *J. Biol. Chem.* **273**, 32763–32770